PROCEEDINGS, 49th Workshop on Geothermal Reservoir Engineering
Stanford University, Stanford, California, February 12-14, 2024
SGP-TR-227

Inferring Zonal Contributions and Productivity from a High-temperature, High-salinity Reservoir

Afrah K. Siddique, D.D. Faulder and Santiago Rocha

Colorado School of Mines, Ryder Scott LP, Cyrq Energy LLC

akasiddique@mines.edu, david_faulder@ryderscott.com, santiago.rocha@cyrqenergy.com

Keywords: Salton Sea, high-salinity, double-diffusive convection, scale, productivity index, mass energy balance, plant process, thermodynamics, total dissolved solids

ABSTRACT

The fluid salinity in a geothermal field is important element in designing a project; the production and injection wellbores, plant thermodynamic processes, and generation capacity. The high-temperature, high-salinity fluid at the Salton Sea Geothermal Field (SSGF) has interesting characteristics used to estimate zonal contribution from wells with two or more producing intervals. In the SSGF it is paramount to develop cost effective well cleanout procedures for the producing wells to remove scale.

Production measurements using orifice meters at the SSGF can have a large error due to the nature of two-phase flow utilizing empirical flow equations and hostile thermo-chemical conditions. This paper describes a correction process that removes noise from the raw production field data, allowing detection of more subtle production, wellhead deliverability, and salinity trends. The field production measurements were corrected using a mass-energy balance (MEB) model of the plant process thermodynamics, variations in wellhead salinity were noted in two wells with one deep production interval and shallower production. The well with only one deep fluid entry showed little or no daily variation in wellhead salinity. This corrected data was used to investigate production well zonal contribution by variations in total produced wellhead salinity. This in turn can be used in estimating zonal contributions and likely zones of wellbore scaling.

This concept was developed further by making a simplifying assumption regarding the vertical reservoir salinity profile based on a double-diffusive convection reservoir process. A linear salinity profile with depth from ~20% TDS at -4000 ft ASL and to ~31% at -8000 ft ASL was assumed to investigate this hypothesis further. Thus, differing production zones depth will have different salinities. This analysis showed consistent relative zonal changes with time as wellbore scale built up in the two wells with two production zones. After each wellbore cleanout cycle, changes in zonal contribution were noted. Additionally, once some estimate of zonal mass contribution is made, a corollary estimate of zonal productivity index (PI) can be made. This method has a significance in inferring productivity from each zone of the production wells improving the productivity of each zone by evaluating the optimum depth, type of cleanouts, frequency, and efficiency of cleanout jobs for producers. This information was used to evaluate and design well scale cleanouts and optimize wellfield operations and capital expenditures.

1. INTRODUCTION

The Salton Sea reservoir contains a high-temperature, high-salinity fluid with productive intervals from approximately -4000 ft ASL to at least -9000 ft ASL. Reservoir temperatures and salinities increase with depth at the top of the high-salinity reservoir from ~500°F and ~20 wt% at approximately -4000 ft ASL to over 600°F and ~31 wt% at -8000 ft ASL and deeper. These productive intervals may be either single fault-dominated entries to multiple entries across several hundred feet. The flowing wells with large mass productivities preclude routine PTS surveys to quantify zonal contribution and changes with time. The production rates are measured using orifice plates, which have a large degree of uncertainty. The daily production rates are adjusted using a comprehensive mass-energy balance (MEB) based on a detailed thermodynamic description of the Featherstone power plant process. After MEB adjustment, it was noted that the wellhead salinity in two wells had daily variations while the third production well had very stable wellhead salinity.

These highly productive wells require routine cleanouts using several methods with hot mud motor cleanouts being one method, Rocha et al. (2023a, 2023b). In the absence of PTS surveys before and after each cleanout, it is difficult to determine how the downhole zonal production has changed. The observation that the MEB adjusted wellhead salinities showed variations suggested that the relative zonal contributions may have changed. Thus, an analytic method was developed to estimate the zonal contributions based on the MEB adjusted wellhead salinity.

2. IMPLEMENTATION OF A MASS-ENERGY BALANCE MODEL

Due to the nature of the Salton Sea brine, empirical calculations for production well measurement using orifice plates result in an observed ±10% errors in mass measurement. A three-stage flash process model was developed to correct the measured raw production rates using the Featherstone power plant thermodynamic process for calibration This section discusses the approach to this problem, how a mass-energy balance (MEB) model was developed, and the PVT behavior of a high-salinity brine.

2.1 Double-diffusive convection in the Salton Sea reservoir

Double-diffusive convection has two requirements for occurrence in a hydrothermal system; the fluid must contain two or more components with different molecular diffusivities in water and these components make offsetting contribute to the fluid density. This results in a high-salinity brine with the same fluid density at all temperatures. Fournier (1990) describes this process conceptually as a series of small scale perturbations of an initially gravity stable system with heating from below. The overlying cooler dilute brine and underlying hotter brine each have convection occurring. As the underlying brine heats from basal heat flow, it causes brine to buoyantly rise into the overlying less dilute brine, creating an intermediate layer of gravitationally stable brine of intermediate salinity and temperature. This process continues through the vertical column reaching a quasi-steady state temperature and salinity profile.

The Salton Sea reservoir has a high-salinity fluid that approaches saturation as the temperature increases with depth. This behavior is best explained by the double-diffusive convective system, Fournier (1990), who noted three key reservoir characteristics. First is decreasing temperature and salinity from the bottom to the top and from the side to the center of the anomaly; second, a very high basal heat flow in the center of the thermal anomaly, in some places much greater than 1000 mW/m^2, requiring a major component of convective heat flow in a chemically stratified reservoir, and third a relatively uniform vertical fluid density throughout the reservoir at all pressure, temperature, and salinity conditions. This last observation implies that although the reservoir fluid is increasing temperature with depth, the fluid density is constant at ~1.0 g/cm^3, first noted by Helgeson (1968). The fluid density was measured five times at one interval in the State 2-14 well to be 1.017 ± 0.0023 g/cm^3 with a median of 0.999 g/cm^3. Additional review from a number of Salton Sea wells Williams and McKibben, (1989), found the hypersaline portion of the reservoir with fluid salinity greater than 20 wt% had a typical range from 0.98 to 1.0 g/cm^3. This requires the fluid salinity to increase with temperature and hence a linear increase in reservoir fluid salinity with depth. This observation meets the conceptual requirements of a double-diffusive convective system where two components make offsetting contribution to the fluid density; decreasing water density being offset by increasing salinity, both as the temperature increases, resulting in a constant density with depth of ~1.0 g/cm^3.

This concept was explored numerically and validated using TOUGH with a simple 2-D cross-sectional model, Oldenburg et al. (1994). The cross-sectional model covered a domain of 2500 m horizontally by 2500 m vertically. No flow boundary conditions were set on the top, bottom and left sides with the right side having a vertical constant fluid density boundary to establish gravity equilibrium in a liquid column with 200°C at the top to 280°C at the bottom. This last condition allows for fluid to enter and leave the model domain only along the right side. Reservoir parameters were chosen to be representative of the Salton Sea reservoir with 20% uniform porosity and vertical permeability set at $5E^{-13}$ m^2 and the vertical permeability 100 times less. The numerical model was allowed to equilibrate to a pseudo-steady-state condition requiring 30 thousand years. It was able to replicate a typical temperature distribution and a uniform brine density of 0.91 to 0.940 g/cm^3, a bit lower than measured. Numerical confirmation of this result was made by one of the authors using TETRAD, which resulted in some adjustment of the equation of state (EOS) brine density to achieve the proper brine density. Both models have a large salinity and temperature gradient in the top 500 m without any lithologic or other reservoir features. It is speculated this is due to the top no-flow and constant temperature (200°C) boundary conditions. The strongly vertical convective flow is diverted horizontally as it nears the top no-flow boundary conditions.

The top of the high-salinity, high-temperature reservoir is generally considered to be around -4000 ft ASL. Temperature mapping at -4000 ft ASL and -6500 ft ASL, **Figure 1**, using initial stabilized temperature survey data from thirty-three wells demonstrates the decreasing temperature from the bottom to the top and from the center to the side of the SSGF. These temperature contours clearly delineates the NE-SW elongate nature of the deep hydrothermal resource and generally correspond to the location of the recent intrusive magma and heat source. They show the eastern side of the SSGF at a lower temperature than the central thermal anomaly, providing hydrologic support such as a constant pressure boundary at a constant fluid density ±1.0 g/cm^3, satisfying a condition for a double-diffusive convection.

The produced fluid from the three production wells analyzed in this study is measured using individual orifice plates for an initial, raw estimate of the two-phase mass rate. One of the problems with two-phase mass rate measurement is that the conversion of upstream pressure and delta pressure through the orifice plate relies proper placement of instrumentation and a complex empirical equation with several choices that can be used, Mubarok et al. (2017). This is further complicated by the high-salinity produced fluid and using orifice plates such that daily data may vary ±10% from MEB corrected production due to pressure taps scaling, flow perturbations due to changing wellbore flow regimes, and well surface interactions through the common production headers to the high pressure separator.

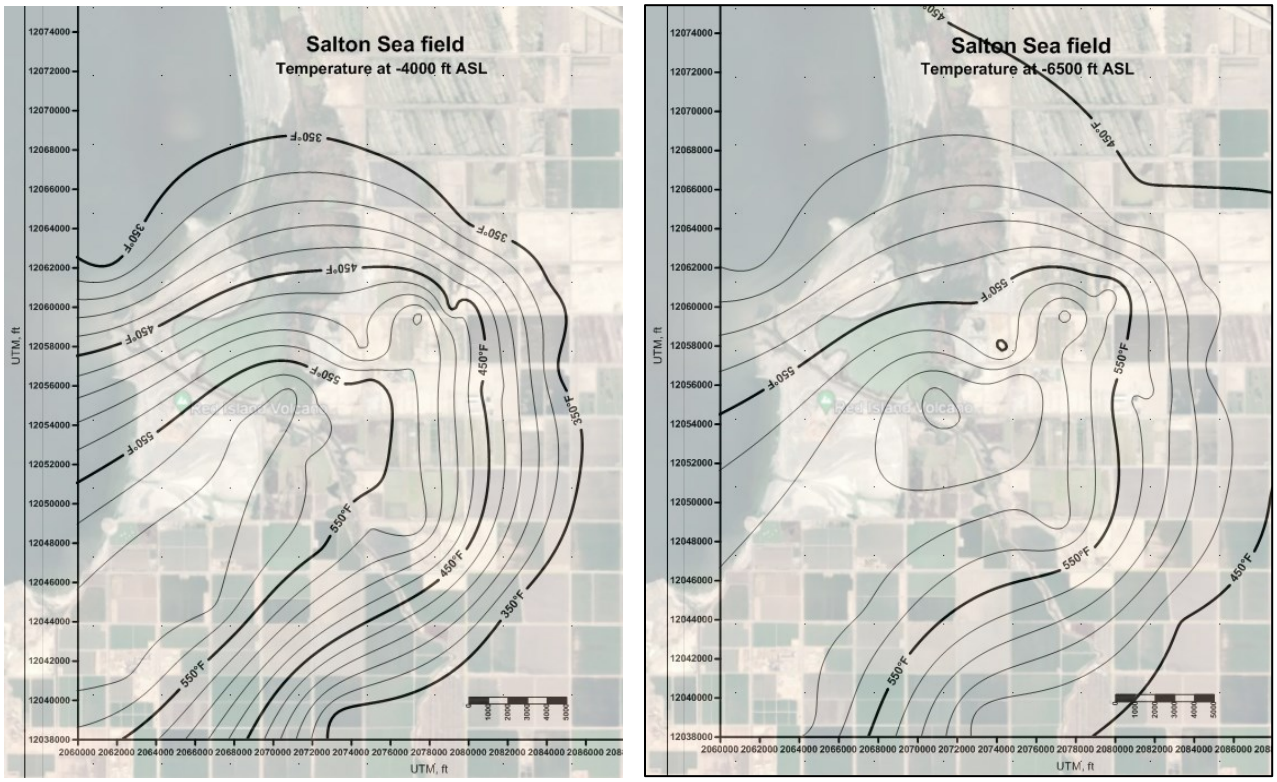

Figure 1: SSGF temperatures at -4000 ft ASL and -6500 ft ASL from thirty-three temperature surveys.

2.2 Mass-Energy Balance (MEB) model

The high-salinity Salton Sea brine has pressure-volume-temperature (PVT) behavior that is different than pure water. Andersen et al. (1992) reviewed the literature and developed PVT correlations that describe fluid behavior at increasing salinities to about 30 wt%. This thermodynamic behavior is described by an excel add-in and was used to develop and calibrate the MEB. It was found this add-in is accurate to about 31 wt%, thus able to describe reservoir and plant thermodynamic conditions. This was key to developing a robust MEB of the field production and power plant processes.

The Featherstone power plant design is a four-stage flash separation (HP, SP, LP and atmospheric), with steam scrubber, dilution water, and crystallizers. The production from three wells are comingle at the high pressure (HP) separator with a design operating pressure of 318 psia with steam wash. The brine underflow undergoes a second-stage flash at 118 psia in the standard pressure (SP) crystallizer with steam wash. The second stage underflow has dilution water added and a third-stage flash at 14 psia in the low pressure (LP) crystallizer and steam wash. The third-stage flash underflow is flashed at atmospheric pressure to heat the dilution water. The steam from the HP, SP, and LP flash enter a three-stage Fuji turbine for power generation. The liquid from the various processes are collected and injected into three wells. The injection rate is measured using high accuracy (0.2 to 1.0%)[1] eddy meters. Gross and net power generation are metered to a very high degree of accuracy, as power sales are the source of project revenue. A simplified process schematic is presented in **Figure 2**.

Analysis of this process schematic shows that the best measured mass and energy values are at the process end, gross and net power generation, **green box**, which is measured to a very high degree of accuracy and the injection rate, **blue box**. Directly measured process parameters, mass rates and pressures, are used to calibrate the MEB. Working upstream through the process, these measured values are used to calibrate the MEB: injection mass rate, HP, SP, and LP steam rates to the turbine, LP crystallizer dilution water mass rate, HP separator and SP/LP crystallizer conditions (steam and brine mass rates, pressure), and the HP separator inlet flow rate. This last is the sum of the three production wells, **red box**, which is the least accurate measurement. The calculated total injection rate is adjusted to equal the measured injection using a production factor to adjust the raw production data, and each well proportional to their raw mass contribution. A second adjustment is made to the HP turbine steam rate so the calculated and measured enthalpy are equal by adjusting the HP separator inlet enthalpy. This two-step adjustment process continues iteratively until the calculated and measure total injection and the HP turbine steam rates are within 0.001 Klbm/hr difference. The calculated single-phase brine enthalpy is within 1 BTU/lbm of enthalpies measured annual using the TFT method. These annual TFT enthalpy measured ground truths the MEB methodology, validating the model.

[1] Krohne Optiflux 4000 magnetic field meters.

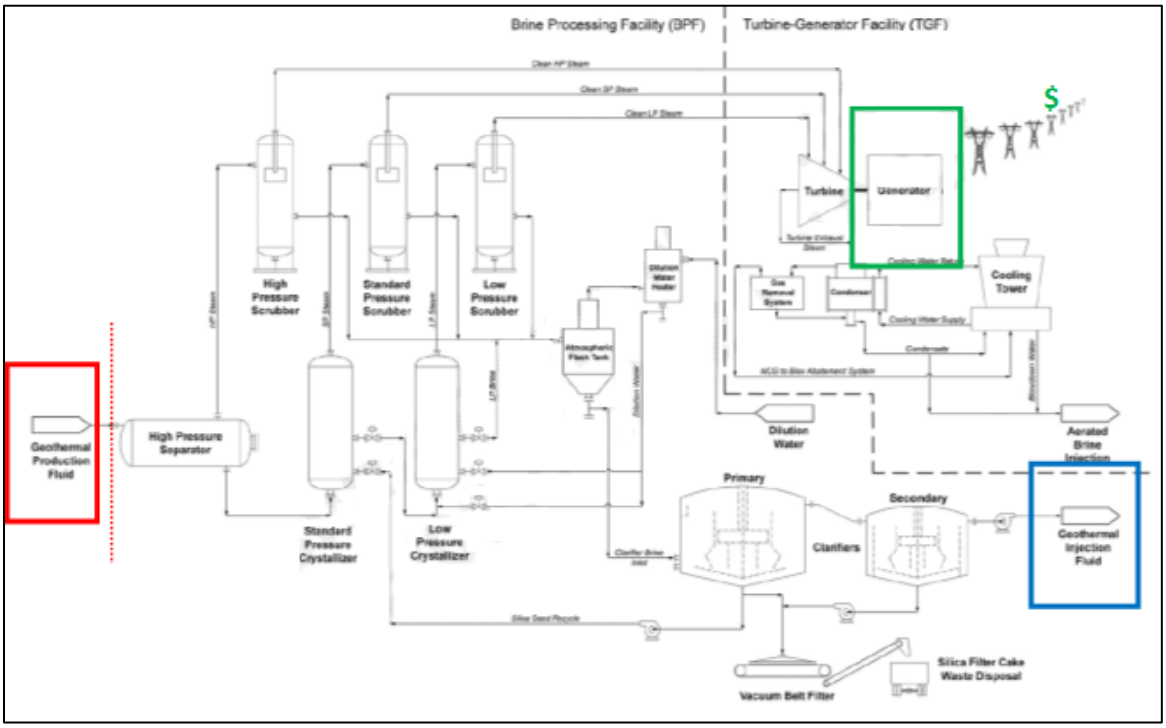

Figure 2: Featherstone power plant simplified process schematic.

A first step was to adjust the wellhead salinity at the measured two-phase wellhead pressure and temperature conditions, 8 to 10% flash, so the calculated temperature is equal to the measured wellhead temperature. The MEB of the power plant process calculates the HP, SP, and LP steam rates and the injection rates and compares this to the measured values. Two key measurements are used to calibrate the MEB model, the turbine HP steam rate which is dependent on the total HP separator brine flow and enthalpy, and the total injection rate which is dependent on the total production mass rate, typically about a 86% injection to production ratio.

The HP separator enthalpy and total mass flow are solved iteratively until the calculated HP turbine steam rate and the total injection rate are within a 0.001 Klbm/hr error tolerance of the measured. This MEB approach used the daily hourly-averaged production data and more interesting, the hourly minute-averaged data showing the diurnal ambient weather impacts. It was found the raw production data measured with orifice plates had a range of ±10% of the final MEB production. Thus, the MEB greatly reduced the uncertainty in production mass measurements. By cleaning up the 'noise' in the raw production data, more subtle trends were observed in the production data and plant process and associated performance metrics. No attempt was made in the MEB to include condenser and cooling tower processes, these were lumped into the total steam usage rate.

Secondary performance metrics can include the turbine steam usage rate, injection-production ratio, brine usage rate, etc. It was found that by taking the noise out of the raw production data, more subtle trends could be identified in these secondary metrics. This was useful identifying which wells are experiencing production decline to scaling, the degree of scaling, and being able to better forecast timing when a well will need a hot mud motor (HMM) cleanout, Rocha et al., (2023a, 2023b)). However, these are limited means to evaluate a scale removal downhole effectiveness without running PTS surveys before and after a HMM and the potential for lost tools.

Upon examining the final data set in detail, it was noted the wellhead salinity for two of the three wells had daily variations and longer term trends. These two wells, A and B, have production intervals in the upper portion of the reservoir and a deeper, fault dominated interval. The well C, did not vary, having only one deep interval, **Figure 3.** This observation and having demonstrated the salinity increases linearly with depth leads to the hypothesis the calculated wellhead salinity could be used to infer well zonal contributions.

The initial data set tested started June 2021, right after a major plant outage. The salinity trend for well A (blue line), is around 0.24 to 0.27 wt% salt. After April 2020 the trend for well C is stable at 0.31 wt%, while well B (red line) showed the greatest variability. The earlier time period has some calibration and measurement errors present, but after the MEB process was implemented, post April 2022 it was possible to identify errant measurements. Usually, this involves rodding out the pressure taps for scale and debris. This later data set was interesting as specific changes in calculated wellhead salinities could be correlated with well scale cleanout operations.

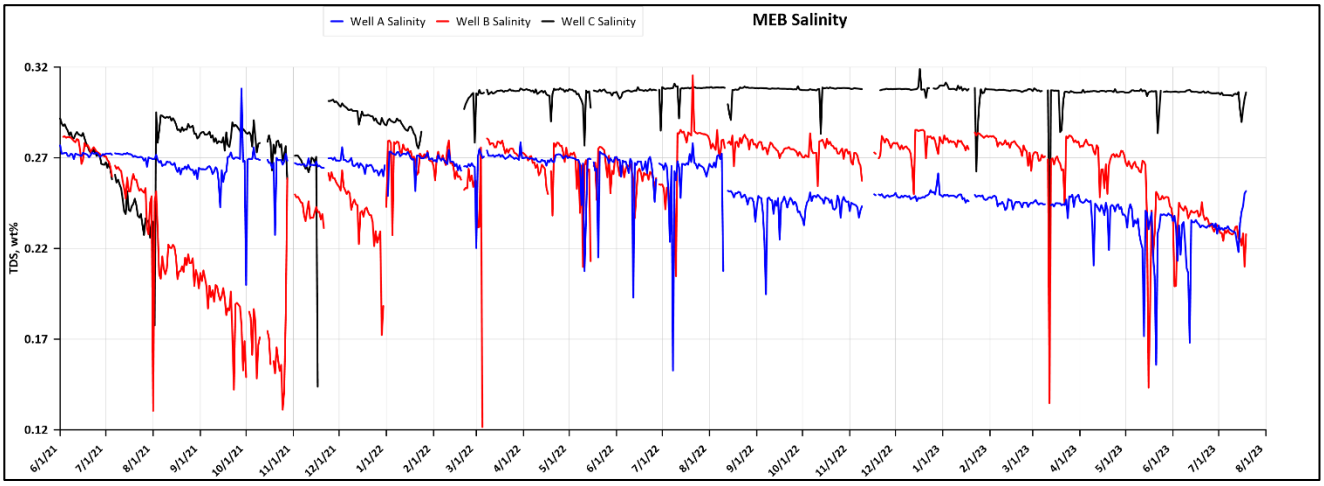

Figure 3: All wells wellhead daily salinity variation

3. WELL ZONAL CONTRIBUTION

The zonal contribution of wells A and B in Hudson Ranch, wells that both produce from multiple zones at different depths was estimated by the variation in the salinity of the total produced fluid at the wellhead. The MEB calculates the salinity of the fluid produced from each well using the measured wellhead pressure and temperature. The salinity estimated for each well producing from several zones can then be used as an input in the simple two-component mixing model. It was found this information could be related to well scale cleanout operations and changes in well zonal contribution and has a direct impact on well cleanout economics.

3.1 Salinity model

The zonal contribution and productivity index of each zone of the producing wells was estimated using an algorithm based on simple two-component mixing model. Salinity with depth varies from about 20% wt% at -4000 ft ASL and up to 31 wt% at -8000 ft ASL at the SSGF, Fournier (1990). We assumed a linear variation of salinity with depth. **Figure 4** shows the assumed linear salinity profile with depth for Salton Sea The salinity gradient for well C salinity was developed using an initial pressure temperature survey and calculate the salinity necessary for a specific gravity of 1.0 g/cm^3.and is compared to the theoretical salinity variation with respect to depth by Fournier (1990).

Well C's downhole salinity concentration is ~30 wt% to 31 wt% from one deep flow zone at -7177 ft ASL which became the basis to re-calculate the salinity variation regarding depth in the zonal contribution calculations. Well C only produces from deeper zone and hence the salinity concentration is stable in comparison to wells. A and B which show variation in salinity concentration based on the combined production from shallower and deeper zones.

Sensitivity was performed on developed algorithm using both salinity gradients for Salton Sea to estimate the zonal contribution and productivity index for producer wells at Hudson Ranch field producing from shallow and the deeper zones. The salinity gradient estimated based on the MEB adjusted wellhead salinity resulted in more realistic estimates of zonal contribution for producer wells. Hence the salinity gradient was used for the zonal contribution calculations.

Sources of error are the assumption that the salinity model is representative and unchanged with time. Injection breakthrough and reservoir mixing could affect the linear model, though no breakthrough has been observed and TFT and model enthalpies are in excellent agreement. Another source is lumping several shallow intervals into one equivalent for model simplicity. A short-term source of error are wellhead temperature and pressure gauges plugging or needing calibration, affecting the wellhead salinity adjustment in the MEB model.

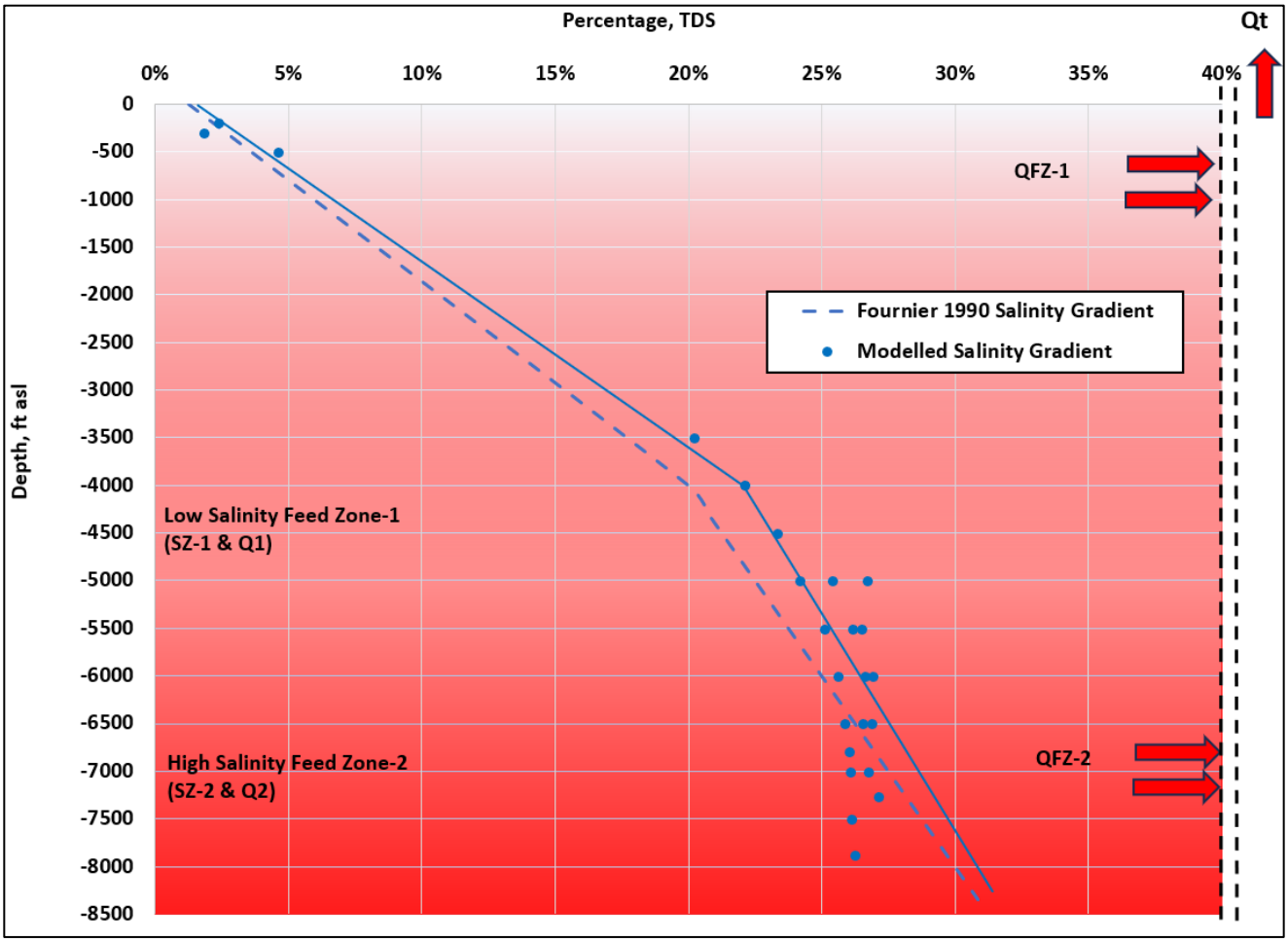

Figure 4: Salinity gradient plot for Salton Sea based on literature and double-diffusive convection model.

3.2 Zonal contribution algorithm

The zonal contribution algorithm was developed based on a simple two-component mixing model. The inputs used for the algorithm are wellhead salinity S_T and total produced flow rate Q_T in Klbm/hr. Wells A and B had discrete shallower production intervals over several hundred feet, these were lumped into an equivalent depth. The deeper, fault dominated was treated as a single interval.

Total wellhead salinity S_T was estimated from MEB model using the PVT add-in. The total produced flow rate, Q_T used the daily production report, which is measured by orifice plates and two-phase correlations, corrected by the MEB model. The equations used to calculate the flow rates Q_{FZ1} and Q_{FZ2} from flow zones FZ-1 (shallower zone ~ Zone-1) and FZ-2 (deeper zone ~ Zone-2) for each well are shown below.

$$Q_{Total} = Q_{FZ1} + Q_{FZ2} \tag{3-1}$$

$$Q_T S_T = Q_{FZ1} S_{FZ1} + Q_{FZ2} S_{FZ2} \tag{3-2}$$

Rearranging the equations above to calculate Q_{FZ1}:

$$Q_{FZ1} = \frac{Q_T S_T - Q_{FZ2} S_{FZ2}}{S_{FZ1}} \tag{3-3}$$

$$Q_{FZ2} = Q_T - Q_{FZ1} \tag{3-4}$$

In the SSGF, Hot Mud Motor (HMM), are needed to successfully clean scale from the wellbore and consequently, restore the productivity of the wells by improving the wellbore geometry Rocha et al.,(2023a). These events were plotted against the calculated zonal contributions in a time series, **Figures 5-6** shows the zonal contribution from wells A and B. It was noted well B had distinct changes in zonal behavior after each HMM cleanout, while the changes in well A were more subdued, yet present. The current model is based on two zones and lumping multiple shallow intervals into one equivalent interval, for the sake of simplicity. One future refinement is to take the lumped data results for the shallower intervals in wells A and B and break out more detail. Notice well B zonal contribution has a lot of noise until about April 2022 when the MEB approach was implemented.

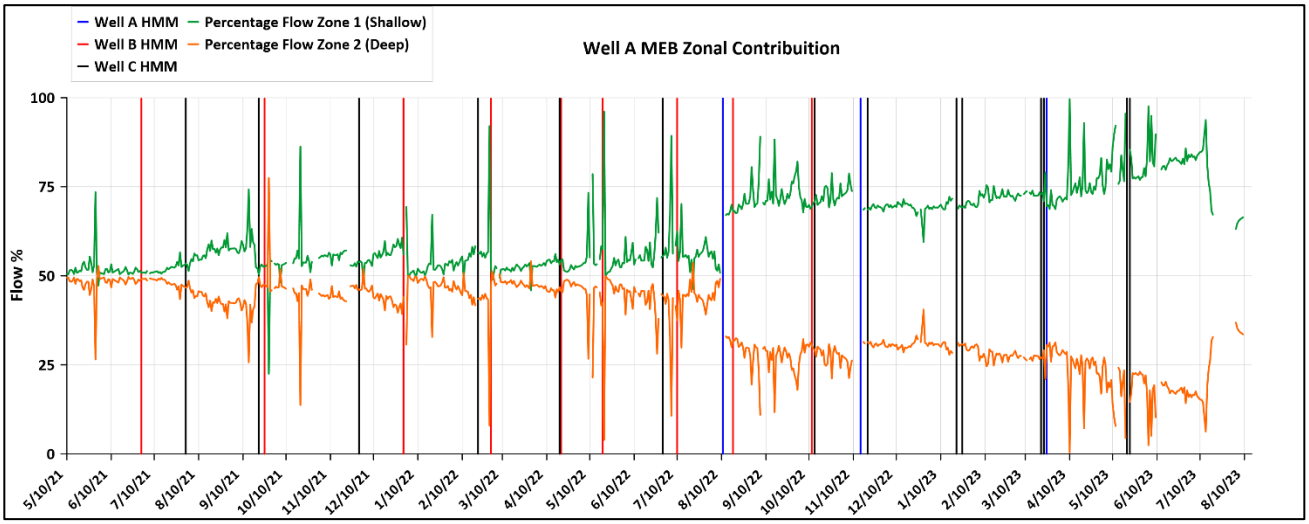

Figure 5: Zonal contribution from well A with reference to cleanout jobs.

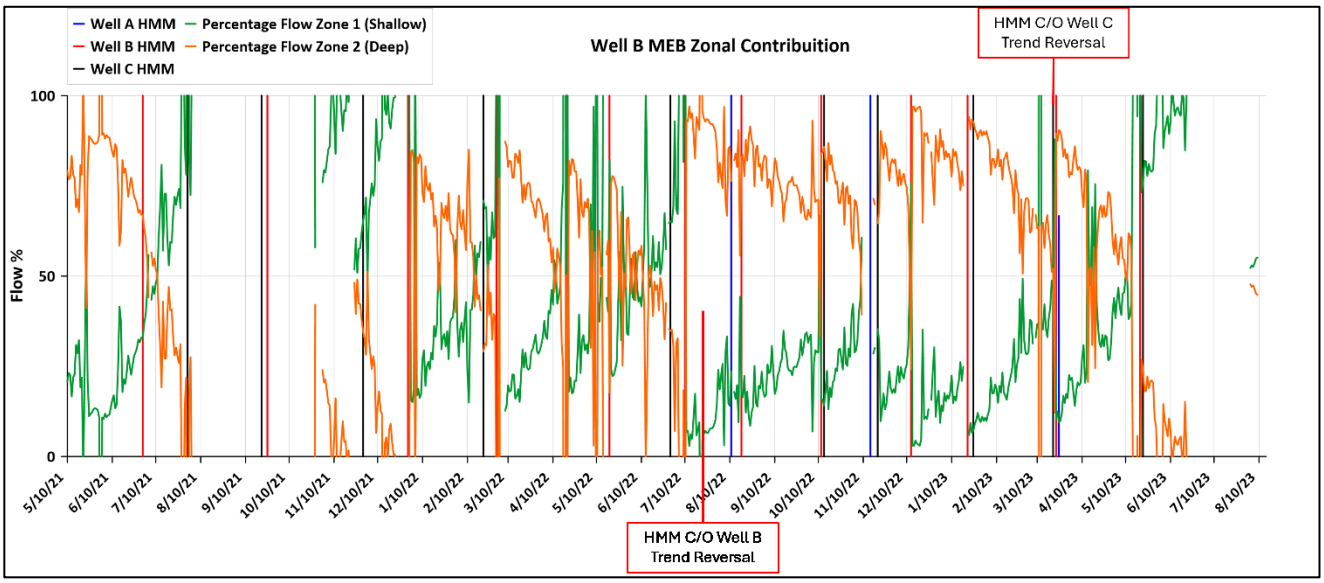

Figure 6: Zonal contribution from well B with reference to cleanout jobs.

3.3 Productivity Index (PI) calculations

Once there is an estimate of the zonal mass contribution, the next step is to estimate the zonal productivity index. The productivity index of each FZ-1 (shallower zone) and FZ-2 (deeper zone) from each well following equation. . The PI requires an estimate of the well flowing pressure, P_{wf} across a fluid entry at a discrete depth, which was obtained by flowing pressure temperature surveys (PTS) and calibrated with WellSim which also provides an independent estimate of zonal PIs. The boundary reservoir pressure, P_{res} is considered as the initial reservoir pressure, as pressure surveillance does not provide any evidence of decline in reservoir pressure. Thus, the same boundary pressure can be used for the entire time series to calculate the PI. This was done for wells A, B and C, **Figure 7**, **Figure 8**, and **Figure 9.**

$$PI = \frac{Mass\ Flow\ Rate\ klbm/hr}{P_{res} - P_{wf}} \tag{3-5}$$

WellSim is used to calibrate flowing PT surveys, with shallower intervals show distinct temperature changes. These are used to calibrate the fluid required at that depth's static temperature by adjusting the zonal productivity index (PI) to match the flowing PT survey. It was found the PI calculated from WellSim was in very good agreement with this method.

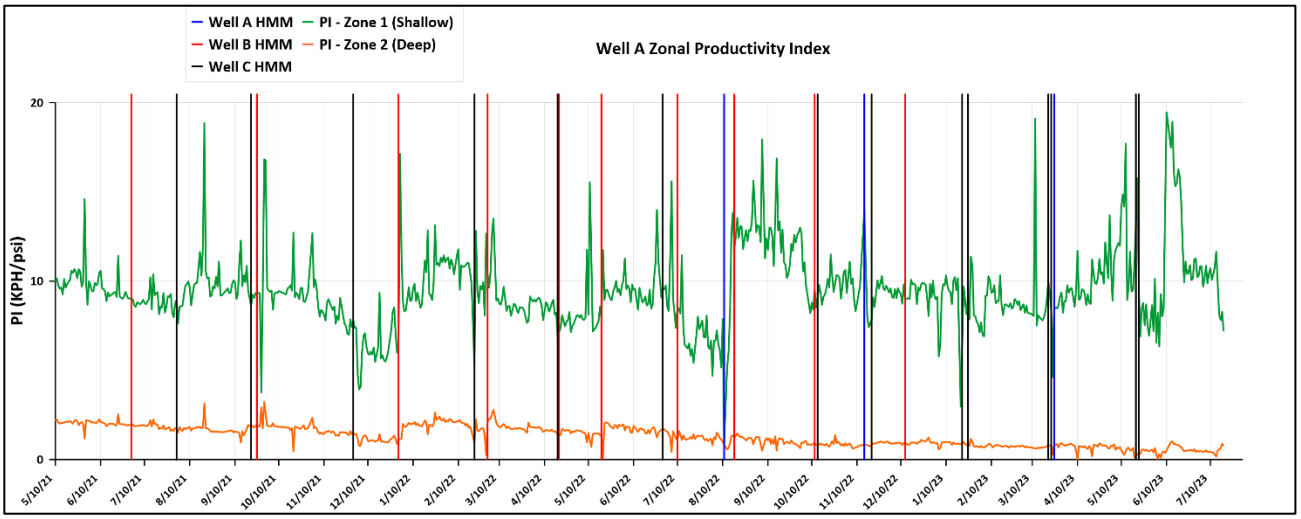

Figure 7: Well A productivity index variation for each zone over time.

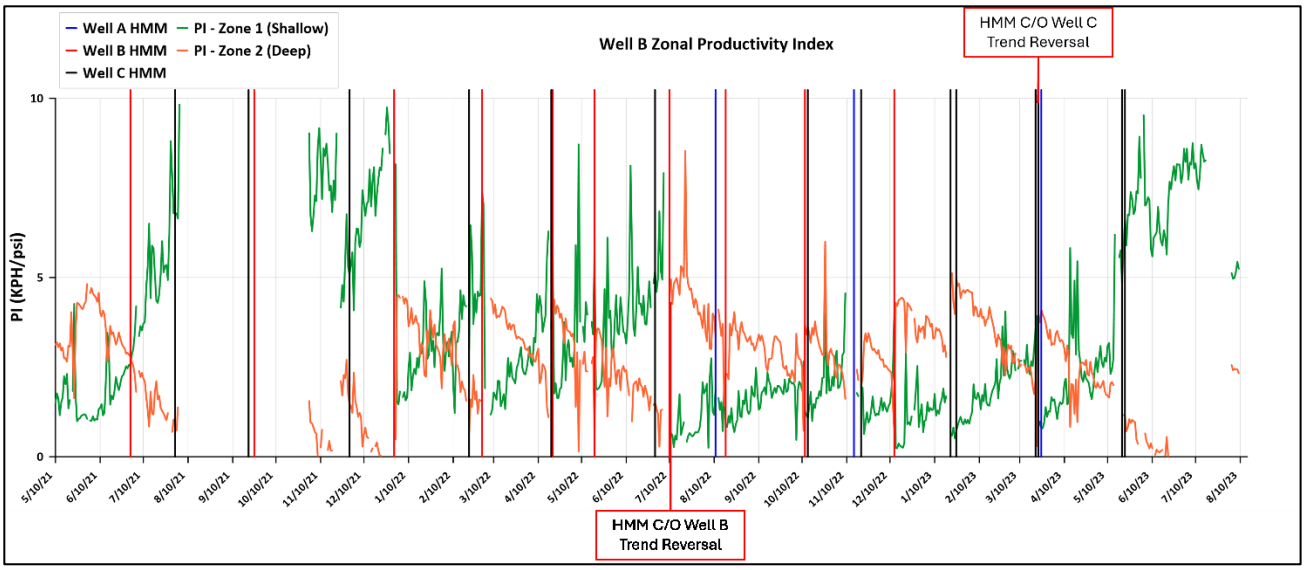

Figure 8: Well B productivity index variation for each zone over time.

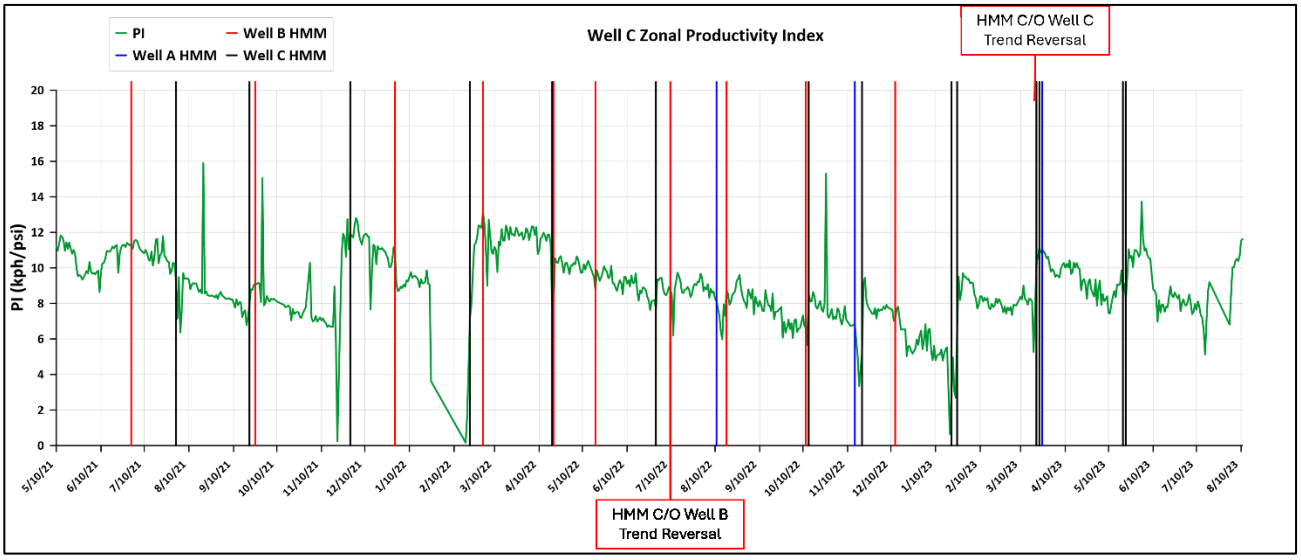

Figure 9: Well C productivity index variation over time.

3.4 Zonal contribution and workover events

Hudson Ranch wells produce high-salinity fluid which creates scale that needs to be regularly removed. For this, systematic cleanout jobs are performed by using a coiled tubing unit with a simple bottom hole assembly that has an all metal motor capable of turning downhole with high fluid temperatures, Rocha et al. (2023a). The zonal contribution algorithm as well as productivity index calculation is useful for estimating the contribution enhancement from each zone of the producer wells after cleanout operations in the cased sections. The main objective of these cleanouts is to remove scale from the shallow sections of the well where most of the scaling is experienced as the fluid is flashing and precipitating scale. This would suggest that the enhancement of flow by removing scale in the shallower portions of the wellbore can modify the zonal contribution deeper in the wells.

The time series plots demonstrate variation in the zonal contribution as well as the productivity of each zone over time. Most of the observed changes, especially the ones on well B were a consequence of HMM operations, regardless of which well was cleaned. This will also suggest that the zonal contribution is changed to a combination of the way the wells are operated on surface, and the reservoir interference between the zones in the wells. For instance, well B experienced trend reversals between its feedzones when well C was cleaned and was producing at higher flowrates and flowing wellhead pressures (FWHP). The deeper zone on well B is located at – 7177 ft, while the only feed zone on well C is located at -7,027 ft. This may suggest that these zones are in communication and that the surface flow and pressure of well C affect the downhole behavior of well B.

Moreover, as the wells produce and scale forms, the zonal contribution from well B tends to overlap, suggesting that the operating FWHP and fluid dynamics in the wellbore are affecting the zonal contribution from the well. When the wells are cleaned again, the deeper feed zones of this well tend to produce more than the shallow ones (higher FWHP and flowrates). This was the case until the cleanouts on well C were modified to allow for better production. From this point, well B started to produce more from the shallow zone. This will suggest that the main driver of the zonal contribution maybe the actual behavior of well C through interaction through the surface production headers.

On the other hand, well A does not show much of an increase in production after cleanout jobs were performed. Most of the changes observed seem to be related to the way the well is being operated. As the well is mainly producing from the highest PI and shallow zone, the well scales less, fewer cleanouts are needed in the well. This work provides engineering guidelines to understand how to improve operations and clean the well.

3.5 Workover Results

The results obtained through the wellhead salinity algorithm led us to understand and estimate the zonal contribution and the productivity index of each zone of the production wells. This in turn supports planning, designing, and executing cost-effective cleanout operations as well as optimal development planning of injection and producer wells to enhance plant efficiency.

Furthermore, it is helpful to interpret these changes in relation to operational modifications and natural events like earthquake etc. It has been observed that higher the FWHP, greater the contribution from the deeper zones which results in higher efficiency in terms of power generation but higher total dissolved solids (TDS) which causes more scaling in the wells due to the complex chemistry of the deeper/saline fluids. The declining FWHP leads to higher contribution from shallower zones which results in lower plant efficiency, and surprisingly, also produces scaling effects due to the lower pressure input from the shallow zones, which leads to shallower flash depths along the wellbore.

4. RESULTS

This effort demonstrated the SSGF reservoir is a double-diffusive convective system with an increase in salinity as temperature and depth increase. This observation leads to a simple linear salinity model with depth profile. A robust thermodynamic mass-energy balance model of the Featherstone power plant was developed and refined using key plant process data. This model was validated and calibrated using key power plant process measurements, then working upstream from the injection rate, the total production mass rate and enthalpy are iteratively calculated and the raw production data adjusted to achieve a mass-energy balance. This greatly reduced the noise in the production and plant process and the technique was extended for hourly data. As part of the MEB methodology, the total wellhead salinity is estimated by the measured pressure and temperature at two-phase conditions.

The daily variations and trends in wellhead salinity in wells A and B were observed, as well as other plant process metrics. The observation of more subtle trends in the wellhead salinity led us to develop a two-component salinity model to infer zonal contributions and PIs. It was noticed that distinct changes in zonal contribution were observed on wells A and B corresponding to well HMM cleanouts, even in those cases where only the cased hole sections were cleaned.

5. CONCLUSIONS

A mass-energy balance model was developed by integrating plant process thermodynamic data and raw production data. This method corrects the raw production data allowing well performance analysis in greater detail, identifying the relative zonal contribution, PI, and changes in productivity with each HMM cleanout cycle. The variation in zonal contribution from each well after every cleanout job dictates the success of the cleanout job, resulting in enhanced production and ultimately the power generation from the plant. Another suggests inferring zonal contribution and pressure interference between the producing zones between the two producing wells. The pressure interference interpreted from zonal contribution calculation is further supported by the geological and geophysical data which

shows that both the wells are drilled in the same block of the faulted compartment of the reservoir. Moreover, this working for zonal contribution and productivity index can also be used as an input for the reservoir simulation model of Hudson Ranch Power I.

ACKNOWLEDGMENTS

The authors would like to thank Cyrq Energy LLC for their support of Ms. Siddique's 2023 summer internship and permission to present these results.

REFERENCES

Andersen, G., Probst, S., Murray, L., and Butler, S: An Accurate PVT Model for Geothermal Fluids as Represented by H2O-CO2-NaCl Mixtures, Proceedings17th Workshop on Geothermal Reservoir Engineering, Stanford University, Stanford, CA (1992).

Fournier, R.O.: Double-Diffusive Convection in Geothermal Systems: The Salton Sea, California, Geothermal System as a Likely Candidate, *Geothermics*, 19, (1990), 481-496.

Helgeson, H.C.:. Geologic and Thermodynamic Characteristics of the Salton Sea Geothermal System, *American J. of Science*, v266, 129-166, (1968).

Mubarok, M.H., Zarrouk, S.J., and Cater, J.E.: The Geothermal Two-Phase Orifice Plate, Proceedings, 39th New Zealand Geothermal Workshop, Rotorua, New Zealand (2017).

Oldenburg, C.M., Pruess, K., and Lippman, M.: Double-Diffusive Convection in Liquid-Dominated Geothermal Systems with High-Salinity Brines, Proceedings19th Workshop on Geothermal Reservoir Engineering, Stanford University, Stanford, CA (1994).

Rocha, S., Faulder, D.D., Capuano, L. III, Capuano, L. Jr., and Walsh, P.: Novel Coiled Tubing Operations in a Hostile Thermo-Chemical Environment, Proceedings, 48th Workshop on Geothermal Reservoir Engineering, Stanford University, Stanford, CA (2023a).

Rocha, S., Faulder, D.D., Capuano, L. III,: Quantifying Scale/Obstruction Thickness in Salton Sea Geothermal Field Wellbores Using Standard Bottom Home Assembly Tools, GRC Transactions, 47, (2023b).

Rook, S.H. and Williams, G.C.: Imperial Carbon Dioxide Gas Field, California Division Oil and Gas, 28th Report, (1942), 23.

WellSim reference manual.

Williams, W.E. and McKibben, M.A.: A brine interface in the Salton Sea geothermal system, California. Fluid and geochemical and isotopic characteristics, *Geochim. cosmochim. Acta,* 53, (1989), 1905-1920.